

Experimental and Numerical Investigations of Transient Natural Convection in Differentially Heated Air-Filled Tall Cavity

Lioua Kolsi^{1,2}, Mohamed Bechir Ben Hamida^{3,4}, Walid Hassen², Ahmed Kadhim Hussein⁵, Mohamed Naceur Borjini², S. Sivasankaran⁶, Suvash C. Saha⁷, Mohamed M. Awad⁸, Farshid Fathinia⁹, Habib Ben Aissia²

¹College of Engineering, Mechanical Engineering Department, Haïl University, Haïl City, Saudi Arabia

²Research Unit of Metrology and Energy Systems, National Engineering School, Energy Engineering Department, University of Monastir, Monastir city, Tunisia

³High School of Sciences and Technology of Hammam Sousse (ESSTHS), Department of Physics, University of Sousse, Sousse, Tunisia

⁴Research Unit of Ionized Backgrounds and Reagents Studies (UEMIR), Preparatory Institute for Engineering Studies of Monastir (IPEIM), University of Monastir, Monastir city, Tunisia

⁵College of Engineering, Mechanical Engineering Department, Babylon University, Babylon City, Hilla, Iraq

⁶Institute of Mathematical Sciences, University of Malaya, Kuala Lumpur, Malaysia

⁷School of Chemistry, Physics and Mechanical Engineering, Queensland University of Technology, Brisbane QLD, Australia

⁸Mechanical Power Engineering Department, Faculty of Engineering, Mansoura University, Mansoura city, Egypt

⁹Faculty of Mechanical Engineering, Universiti Teknologi Malaysia, UTM Johor Bahru, Malaysia

Email address:

lioua_enim@yahoo.fr (L. Kolsi), benhamida_mbechir@yahoo.fr (M. B. B. Hamida), hassen.walid@gmail.com (W. Hassen), ahmedkadhim7474@gmail.com (A. K. Hussein), borjinimn@yahoo.com (M. N. Borjini), sd.siva@yahoo.com (S. Sivasankaran), suvash.saha@qut.edu.au (S. C. Saha), m_m_awad@mans.edu.eg (M. M. Awad), ffarshid2@live.utm.my (F. Fathinia), habib_enim@hotmail.fr (H. B. Aissia)

To cite this article:

Lioua Kolsi, Mohamed Bechir Ben Hamida, Walid Hassen, Ahmed Kadhim Hussein, Mohamed Naceur Borjini, S. Sivasankaran, Suvash C. Saha, Mohamed M. Awad, Farshid Fathinia, Habib Ben Aissia. Experimental and Numerical Investigations of Transient Natural Convection in Differentially Heated Air-Filled Tall Cavity. *American Journal of Modern Energy*. Vol. 1, No. 2, 2015, pp. 30-43.

doi: 10.11648/j.ajme.20150102.12

Abstract: The two-dimensional laminar natural convective transient flow characteristics in a differentially heated air-filled tall cavity with gradual heating are investigated both experimentally and numerically for various parameters such as Rayleigh number and temperature difference. Experimental computations are performed for temperature difference varying from ($\Delta T = 5^\circ\text{C}$) to ($\Delta T = 23^\circ\text{C}$) while the Rayleigh number varies from ($Ra = 2929$) to ($Ra = 11772$) to cover a wide range of the flow field inside the cavity. The results show that as the Rayleigh number increases the flow becomes unstable. Also, the flow characteristics are observed to be multi-cellular and time variant especially at high Rayleigh numbers. Moreover, numerical computations are performed to compare with the experimental results.

Keywords: Natural Convection, Tall Cavity, Experimental Investigation, Transient, Gradual Heating

1. Introduction

Natural convection flow and heat transfer in cavities or enclosures has been extensively studied in past decades regarding the numerous applications in several industrial fields. Examples include electronic devices cooling, lubrication technologies, food processing, float glass production, flow and heat transfer in solar ponds,

thermal-hydraulics of nuclear reactors and solar collectors. Natural convection flows are particularly difficult to control because they depend on various factors such as the geometry, fluid thermo-physical properties etc. [1-2]. A huge amount of studies were presented in the literature especially regarding cavities with different shapes and boundary conditions. While the numerical methods allowed a complete description of the flow and thermal fields inside the cavity, it was still

limited to find a complete experimental analysis of the cavity in the available literature, especially which were treated with tall cavities. For more details about natural convection in cavities with various conditions, an extensive literature review has been done by Fusegi and Hyun [3] and Khalifa [4-5], considering spatial and temporal variations of thermal boundary conditions, variable properties effects and multi-dimensionality. Turner and Flack [6] performed experimental measurements of natural convective heat transfer in rectangular enclosure with concentrated energy sources. They analyzed the temperature field in it through a Wallaston prism Schlieren interferometer. Fills and Poulikakos [7] performed an experimental study of natural convection in a parallelepiped enclosure induced by a single vertical wall. The upper half of this wall was warm while the lower half was cold. The other enclosure walls were considered insulated. The temperature and flow measurements were performed in the high Rayleigh number regime ($1010 < Ra < 5 \times 1010$) by using water as working fluid. The flow field featured two flat cells, one filled with warm fluid along the top horizontal wall, and the other filled with cold fluid along the bottom horizontal wall. Tanasawa [8] presented some experimental techniques in natural convection heat transfer. The techniques were mostly related flow visualization, temperature field, and heat flux distribution in fluids. Three topics were presented, the first being natural convection in a horizontal rectangular liquid layer driven by surface tension and buoyancy. The second topic was the onset of oscillatory convection in the Czochralski growth melt. The third topic was the rollover of double liquid layers that were stratified stably due to a density difference. He emphasized the importance of visual observation in the investigation of natural convection phenomena. Ramos and Milanez [9] performed experimental and numerical investigations of the natural convection in cavities heated from below by a heat source, which dissipated energy at a constant rate. Salat et al. [10] investigated experimentally and numerically the turbulent natural convection flow in a differentially heated cavity of height ($H = 1$ m), width ($W = H$) and depth ($D = 0.32H$), submitted to a temperature difference between the active vertical walls equals to 15 K resulting in a characteristic Rayleigh number equals to (1.5×10^9). Numerical simulations were performed for both adiabatic conditions and experimentally measured temperature on the horizontal walls. Bae and Hyun [11] carried out a numerical study of the transient convection in rectangular and elongated cavities with a hot wall composed by three heated bands. They presented the temperature evolution for Rayleigh number in the range 105–107 and the analysis of the inner flow through the streamlines and temperature distribution as a function of the dimensionless time. Laguerre et al. [12] carried out an experiment using a refrigerator model in which heat was transferred by natural convection between a cold vertical wall and the other walls, which were exposed to heat losses. The air temperature profile in the boundary layers and in the central zone of the empty refrigerator model was investigated. Temperature

stratification in the vertical direction was observed with the cold zone at the bottom and warm zone at the top of the cavity. Corvaro and Paroncini [13] performed a numerical and experimental analysis to study the natural convection heat transfer in a square cavity heated from below and cooled by the sidewalls. The enclosure was filled with air and a discrete heater was mounted on its lower surface. The air temperature distribution and the Nusselt numbers at different Rayleigh numbers were measured by a holographic interferometry and the double-exposure technique. A 2D particle image velocimetry (PIV) was utilized to measure the velocity fields at the same Rayleigh numbers. Experimental and numerical correlations were determined for each position analyzed to connect the Rayleigh numbers with the Nusselt numbers. Laguerre et al. [14] performed an experiment using a refrigerator model in which heat was transferred by natural convection. This transfer occurred between a cold vertical wall and the other walls, which were exposed to heat losses. The air velocity measurements were undertaken using a Particle Image Velocimetry (PIV). Circular airflow was observed in the cavity where air moved downward along the cold wall and upward along the other walls. It was found that the influence of the cold wall temperature on the air velocity was more significant than the surface area. Corvaro and Paroncini [15] provided an experimental analysis of the natural convection in a differentially heated side square enclosure. The cavity was full of air and was heated by a hot wall. The effect of the position of this source on the dynamic structures generated by the natural convection heat transfer was analyzed at the steady state and under laminar conditions. The experimental apparatus was a 2D-PIV system while the experimental data consisted of vector maps, velocity maps and streamlines at different Rayleigh numbers. During their study the presences of two small vortices was noticed on the upper surface of the source and were dependent both on the Rayleigh numbers and on the position of the heater. Jeng et al. [16] performed both experiments and numerical works to study transient natural convection flow and transport process due to mass transfer in inclined enclosures. In the experiments, the enclosure was filled with aqueous solution where the flow structure was visualized by both particle tracer and shadowgraph. Two opposed sidewalls of the enclosure were maintained at different concentrations while the other sidewalls were considered insulated and impermeable to the species transfer. During the experiments, the Rayleigh number ranges from 1.126×10^8 to 1.157×10^{11} , the angles of inclination from 30 to 90° and the enclosure aspect ratio from 0.6 to 1. Corvaro et al. [17] presented a PIV and Holographic interferometry measuring on natural convection in a square enclosure filled with air. Two temperatures (cold and hot) were applied on the vertical sides of the enclosure. Tests involved three different configurations, with the hot part in the middle of one wall, and the cold part at the bottom, in the middle or at the top of the opposite wall. For each configuration measurements were performed with different temperatures of the hot wall. Velocity maps, streamlines maps and interferograms were

presented. Results showed that the configuration with the cold part at the top of the wall produced the fastest dynamic field and the highest Nusselt number. Saury *et al.* [18] built and instrumented large-scale experimental setup which consisted in a 4 m-high cavity with a horizontal cross-section equals to $(0.86 \times 1.00 \text{ m}^2)$. Two opposite vertical walls were heated and cooled down while the other walls (lateral walls, ceiling and floor) were made of insulating medium covered with a thin and low-emissivity film designed to minimize radiative effects into the cavity. The temperatures of active walls were imposed, constant and equally distributed around the ambient temperature in order to reduce heat losses. The temperature difference between the hot and cold walls was chosen to respect the Boussinesq approximation. Under the considered assumptions, Rayleigh number values up to 1.2×10^{11} ($\Delta T = 20 \text{ }^\circ\text{C}$) could be obtained. Also, the airflow inside the cavity was analyzed and the Nusselt number along the hot and the cold wall was presented. Another useful researches have been conducted about this subject under different conditions can be found in [19–26]. Multi-cellular flows in two-dimensional high aspect ratio cavities, such as those encountered in insulated glazing units, are the main focus of the present work. To the best knowledge of the authors and depending on the previous literature review, there are a few researches deals with the experimental investigation of transient natural convection in a two-dimensional differentially heated air-filled elongated cavity. The focus in most experimental and computational work is on small aspect ratio cavity. The main purpose of the present work is limited to vertical air filled tall cavities. Therefore, this work is a good attempt to fill this gap and deals with this restricted subject.

2. Experimental Apparatus

2.1. Experimental Arrangement

The experimental model designed for the study of natural convection is described in this section. Experiments were made in order to study the flow in a vertical geometry (differentially heated vertical cavity). The design requirements are:

- 1- A high aspect ratio;
- 2- Leave a transparent space in order to visualize the flow;
- 3- A perfect seal which allows working with different fluids;
- 4- The two vertical cavity walls are perfectly isothermal while the other walls are adiabatic.

A schematic diagram of the experimental apparatus is presented in Fig.1. The vertical right and left walls of the cavity are composed from two aluminum plates of (60 cm) long and (30 cm) wide (with an effective length of 29.5 cm). The distance between the two walls is (1.9 cm), so the aspect ratio is about 15.5. Each vertical walls (differentially heated walls) is composed of two plates, the first is Plexiglas with a thickness of (1cm) and the other is Aluminum (Al Cu 4mg Si) characterized by a thermal conductivity $k = 134 \text{ W/ m. K}$ at ($25 \text{ }^\circ\text{C}$) with a thickness of (2 cm). These two walls are protected by an insulator which has a thickness of (2 cm) in order to limit the heat exchange with the external environment. The differentially heated walls create buoyancy driven convection inside the cavity. To be sure to have fully isothermal walls, a thermal regulation by thermostated baths is used. Several channels were milled on the two aluminum walls in order to circulate constant temperature water provided by the thermostated baths. For each wall, there are two collectors which allow a fair supply of water in the different channels.

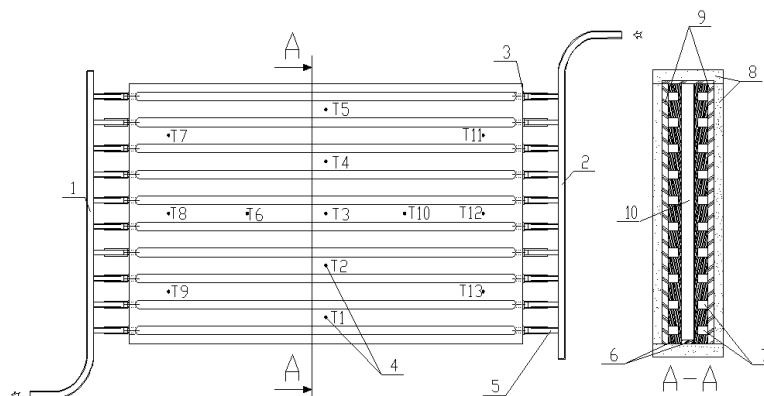


Figure 1. Schematic of the experimental setup.

- 1 : Fluid outlet manifold
- 2 : Fluid inlet manifold
- 3 : Nozzles supply
- 4 : Thermocouples
- 5 : Flexible connector
- 6 : Aluminum plates
- 7 : The grooves on the aluminum plates
- 8 : Insulation
- 9 : Plexiglas
- 10 : Cavity

2.2. Thermal Regulation of the Installation

As mentioned above the thermal regulation is done by thermostated baths to ensure a constant temperature of each of the aluminum plates. The grooves in each of the two walls, allow the circulation of the heat transfer fluid. To have a differentially heated cavity we use two thermostated baths, one for controlling the temperature of the cold water and the other for the hot water. These thermostated baths have the following characteristics:-

- 1- Volume: 40 liters.
- 2- Materials: (1 cm) layer of Plexiglas and an insulation layer of (2 cm).
- 3- Thermo-regulator: POLYSTAT CC2 nominal power (2000 W).
- 4- Flow: Between (7-10 liters / minute).
- 5- Temperature: From ambient to 200°C.
- 6- Precision error: ± 0.1 °C.

In order to verify the uniformity of the temperature field in both aluminum walls, 13 type-T thermocouples are implemented on each of these walls as shown in Fig.1. Moreover, to be able to measure the internal temperature of the plates accurately, these thermocouples are placed at a distance of (1 mm) from the internal surface. The acquisition of the temperatures is carried out using a data logger (SCB 68 Mio-16 E) Series which is capable of managing up until 16 thermocouples simultaneously. The data logger is connected to a computer and has the following advantages:

- 1- Ability to choose and select the acquisition frequency from data management software.
- 2- It has a storage capacity of more than 10 000 measurements.

The flow visualization is made using a camera-type TM 1300, with a resolution of (1280 x 1340) and a frequency of 12 frames per second. To view the central plane of the cavity, a laser generator and an optical system consisting of a plane mirror and a semi-cylindrical lens whose aim is to produce a thin laser plane were used. Before the start of the thermostated baths that will create differentially heated walls, the Smoke (considered as a tracer) which allows the visualization of the flow at the central plane of the cavity is introduced. The steps of visualization are as follows:

- 1- Introduction of the smoke into the cavity.
- 2- Adjustment of the laser plane with the central plane of the cavity.
- 3- Adjustment and positioning of the camera.
- 4- Starting of thermostated baths and acquisition board.
- 5- Waiting for steady state, then begins recording data.

The temperature of the cold thermostatic bath is maintained at 30°C, while the temperature of the hot wall is gradually raised to the desired set point. Indeed, the heating of the bath is done first without external circulation of the regulate fluid and when the desired temperature is reached the pump turns on. Fig. 2 shows a real picture of the experimental apparatus, while Fig. 3 shows a schematic diagram of the measuring instruments and data acquisition.

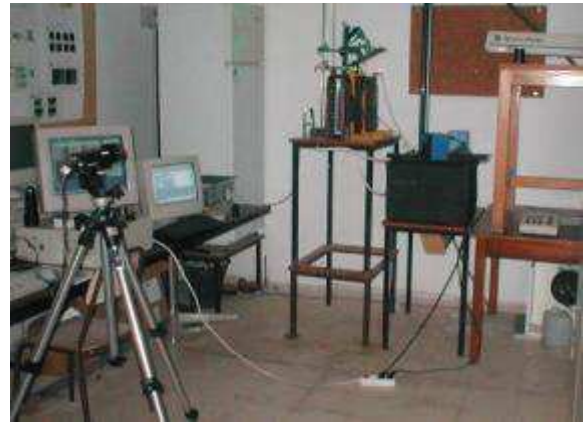


Figure 2. Real picture of the experimental apparatus.

3. Mathematical Model and Numerical Solution

The physical system consists of a rectangular enclosure with $H/W = 15$ as aspect ratio and with uniform imposed temperatures along the left and right vertical walls. The top and bottom of the enclosure are assumed to be adiabatic.

It is assumed that the flow in the system is laminar with no-slip conditions at the walls, the physical properties are constant, and the Boussinesq approximation is valid.

The stream function-vorticity formulation is used to express the governing equations for the laminar and unsteady state natural convection:

Scaling length, velocity and time by W , α/W and W^2/α , and defining dimensionless temperature as $T = (T' - T'_c) / (T'_h - T'_c)$, the governing equations in dimensionless stream function-vorticity form are:

Vorticity

$$\left(\frac{\partial \omega}{\partial t} + u \frac{\partial \omega}{\partial x} + v \frac{\partial \omega}{\partial y} \right) = \text{Pr} \left(\frac{\partial^2 \omega}{\partial x^2} + \frac{\partial^2 \omega}{\partial y^2} \right) + Ra \text{Pr} \frac{\partial T}{\partial x} \quad (1)$$

Energy

$$\left(\frac{\partial T}{\partial t} + u \frac{\partial T}{\partial x} + v \frac{\partial T}{\partial y} \right) = \left(\frac{\partial^2 T}{\partial x^2} + \frac{\partial^2 T}{\partial y^2} \right) \quad (2)$$

Kinematics

$$\omega = - \left(\frac{\partial^2 \Psi}{\partial x^2} + \frac{\partial^2 \Psi}{\partial y^2} \right) \quad (3)$$

The foregoing dimensionless parameters are given as follows:

$$\text{Pr} = \frac{\nu_f}{\alpha_f} \quad \text{and} \quad Ra = \frac{g \beta_f \Delta T W^3}{\nu_f \alpha_f}$$

The associated initial and boundary conditions for the problem considered are:

For $t \leq 0$:

$$\omega = \Psi = \frac{\partial \Psi}{\partial x} = \frac{\partial \Psi}{\partial y} = T = 0 \quad (\text{everywhere})$$

For $t > 0$:

$$\text{On the vertical left wall}(x=0): \Psi = \frac{\partial \Psi}{\partial x} = T = 0 \quad ; \quad T = 1$$

$$\text{On the vertical right wall}(x=1): \Psi = \frac{\partial \Psi}{\partial x} = T = 0 \quad ;$$

$$\text{On the horizontal walls: } \Psi = \frac{\partial \Psi}{\partial y} = \frac{\partial T}{\partial y} = 0;$$

Experimental studies often report the wave number (α) based on the wavelength (λ) of the cells or vortices which is given by:

$$\alpha = 2\pi / \lambda \quad (4)$$

The mathematical model described above was written into a FORTRAN program. The control volume finite difference method is used to discretize governing equations [1-4]. The central-difference scheme is used for treating convective terms while the fully implicit procedure is used to discretize the temporal derivatives. The grids are considered uniform in all directions with additional nodes on boundaries. The successive relaxation iteration scheme is used to solve the resulting non-linear algebraic equations. The time step (10^{-5}) and spatial mesh (21×301) are utilized to carry out all the numerical tests. The solution is considered acceptable when the following convergence criterion is satisfied for each step of time:

$$\sum_i^{1,2,3} \frac{\max |\psi_i^n - \psi_i^{n-1}|}{\max |\psi_i^n|} + \max |T_i^n - T_i^{n-1}| \leq 10^{-5} \quad (5)$$

4. Results and Discussion

Figure 4 shows the variation of walls temperatures with time for three different temperature difference which are respectively ($\Delta T = 5^\circ\text{C}$), ($\Delta T = 10^\circ\text{C}$) and ($\Delta T = 15^\circ\text{C}$). It is observed that the temperatures increase when the time increases until it reach the steady state regime after about (80 min). Moreover, it can be noticed also from the same figure, that the temperature increases when the temperature difference increases from ($\Delta T = 5^\circ\text{C}$) to ($\Delta T = 15^\circ\text{C}$). Figures 5 and 6 present the flow patterns produced experimentally after flow visualizations for various temperature variations which are ($\Delta T = 5^\circ\text{C}$), ($\Delta T = 10^\circ\text{C}$), ($\Delta T = 10.5^\circ\text{C}$) and ($\Delta T = 11^\circ\text{C}$) and Rayleigh number varies as ($Ra = 2929$), ($Ra = 5635$), ($Ra = 5889$) and ($Ra = 6147$) [Fig. 5] and ($\Delta T = 11.5^\circ\text{C}$), ($\Delta T = 12^\circ\text{C}$), ($\Delta T = 12.5^\circ\text{C}$) and ($\Delta T = 13^\circ\text{C}$) while Rayleigh number varies as ($Ra = 6397$), ($Ra = 6651$), ($Ra = 6904$) and ($Ra = 7153$) [Fig. 6]. It can be observed the generation of convection vortices and its intensity increases as the Rayleigh number increases due to the significant effect of convection when the Rayleigh number increases. When buoyancy force becomes greater than the viscous force, the natural convection in the tall cavity becomes dominating. Due to the buoyancy force, the flow pattern begins to move

from the hot cavity sidewall and then arrives to the adiabatic upper wall. After that, the flow pattern moves towards the other cold cavity sidewall and finally reaches the adiabatic lower wall. This motion leads to generate the convection rotating vortices which depend on the motion of air due to the differentially heated sidewalls. When the Rayleigh number is low ($Ra = 2929$) as shown in Fig. 5, the flow is laminar, slowly ascending near the hot wall and slowly descending near the cold wall. The flow circulation is poor due to the slight effect of convection currents at low Rayleigh number. In this case, no fluctuations are observed, meaning that the flow is unicellular. But, as the Rayleigh number increases, the vortices become strong and can be clearly visible especially at ($Ra = 7153$). Furthermore, the vortices begin to elongate vertically inside the cavity zone as the Rayleigh number increases. The air circulation inside the cavity is highly dependent on Rayleigh number where a circulation flow region of high intensity can be observed adjacent to the hot wall and tries to push the air towards the cavity core. Moreover, it can be noticed that the nature of the flow instability changes with increasing temperature difference. Figures 7, 8 and 9 present respectively the sequence of the flow growth produced experimentally inside the cavity after flow visualizations for $Ra = 7402$ ($\Delta T = 13.5^\circ\text{C}$), $Ra = 8141$ ($\Delta T = 15^\circ\text{C}$) and $Ra = 11772$ ($\Delta T = 23^\circ\text{C}$). The results show that for Rayleigh numbers below $Ra = 7402$ ($\Delta T = 13.5^\circ\text{C}$) the flow pattern is permanent and approximately wavy. Also, a clear deformation can be detected in the core vortices. For Rayleigh numbers higher than 11772 ($\Delta T = 23^\circ\text{C}$) the flow pattern becomes unstable and no reverse transition can be observed. For further increasing in the Rayleigh number, the regularity of the oscillations is destroyed and the multi-cellular laminar flow being fully established, before becoming turbulent. It is interesting to mention that most authors observe a cat-eye pattern in flow for high aspect ratios or high form factor ($H > 12$) that then transitions to a traveling wave instability. In this work, the cat-eye pattern occurred as expected and becomes traveling waves for $Ra = 11772$. This observation gives a good verification of the measured results. Figure 10 shows the numerical results of flow field contours inside the cavity for gradual heating at $H = 15.5$, $Pr = 0.7$ for various Rayleigh number ranging from $Ra = 7000$ to $Ra = 25000$. It can be noticed from the figure that as the Rayleigh number increases the core of vortices increases due to the significant effect of natural convection and begin to deform and move towards the central part of the cavity. Furthermore, it can be concluded from this figure that the flow vortices shape becomes non-monotonic as the Rayleigh number increases. In addition, it can be observed from Fig. 10, that there is a space region in the core of the cavity. This is due to the stagnant or low fluid velocity. From the other hand, the numerical results show that the flow is carried out from the hot wall towards the cold one along the upper horizontal plate. This prediction agrees with the experimental results. Moreover, it can be observed from Fig. 10, the existence of the multi-cellular flow called secondary flow. It is useful to mention that the linear stability analyses predict a row of co-rotating secondary cells as indicated in

Pons [27].

The secondary cells are long in the vertical direction and small in the horizontal direction. The advantages of the secondary cells are to reduce the friction effect in the core of the cavity; reduces the boundary layers against the vertical walls, and to re-circulate the fluid inside the cavity. Therefore, the numerical results are very necessary to verify the

experimental results for cavities with a high aspect ratio. Figure 11 is presented to show the wave length of the vortices which is required for experimental studies. This figure shows that the size of the secondary cells can be measured as the vertical center distance between adjacent cells.

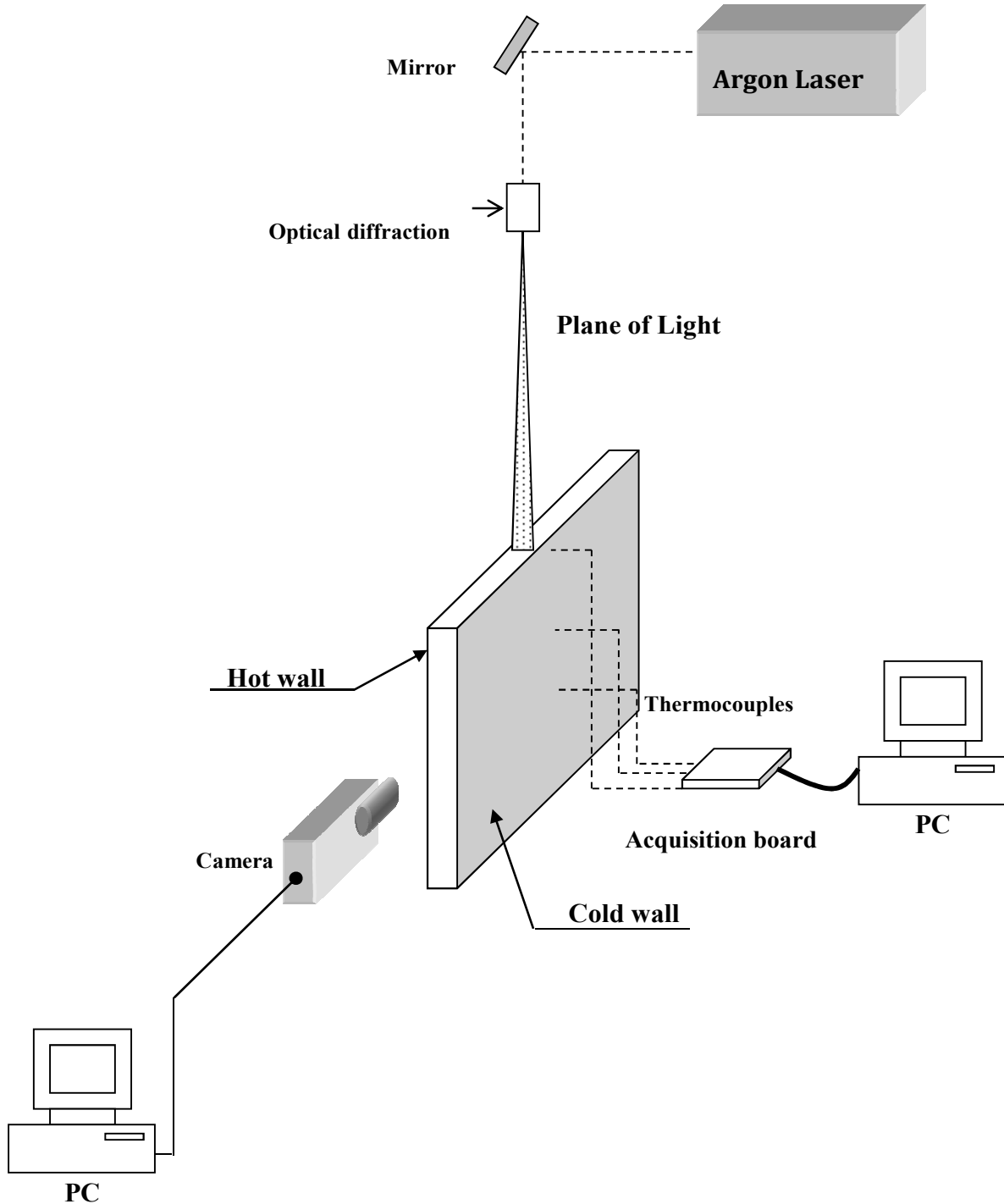


Figure 3. Schematic of the measuring instruments and data acquisition.

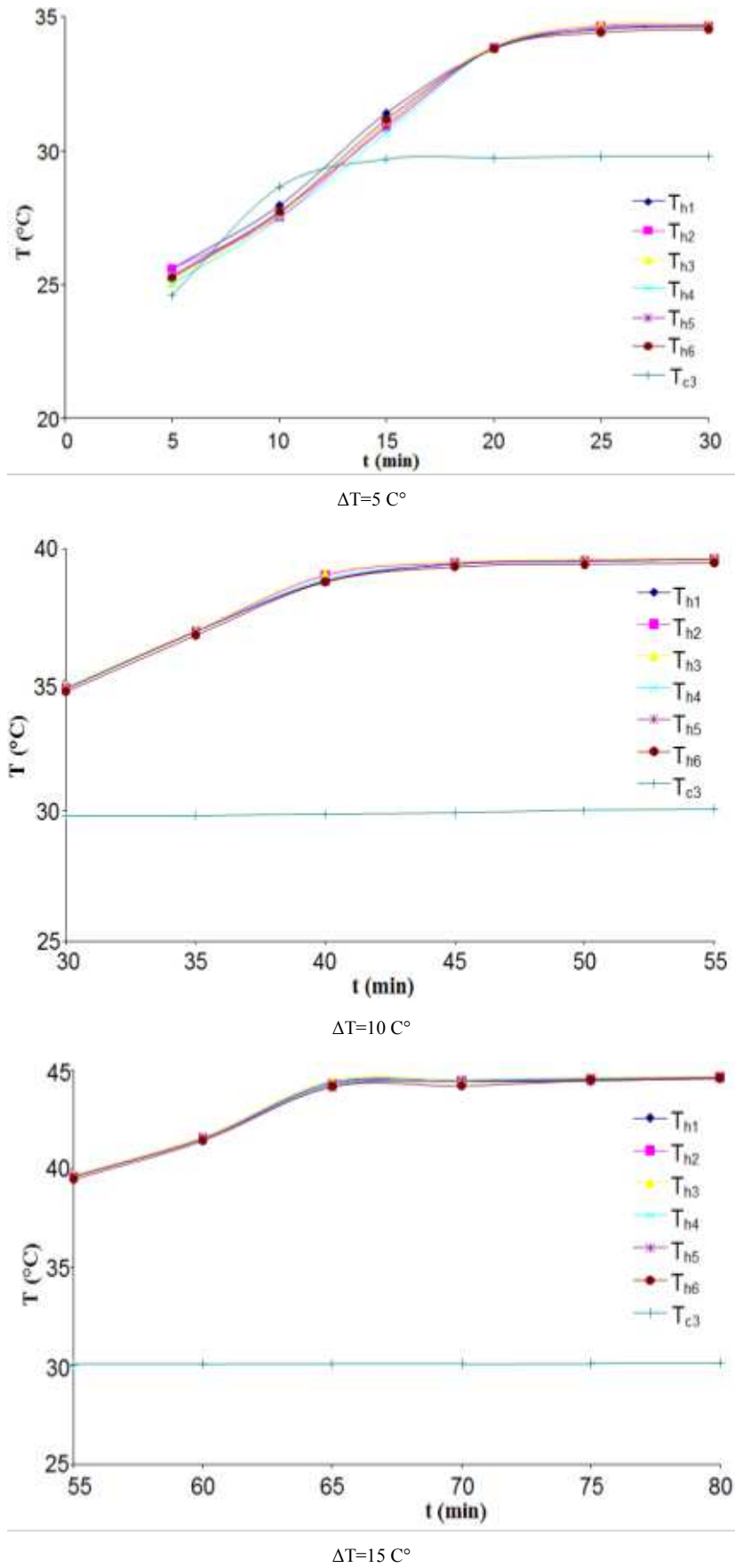


Figure 4. Variation of walls temperatures with time.

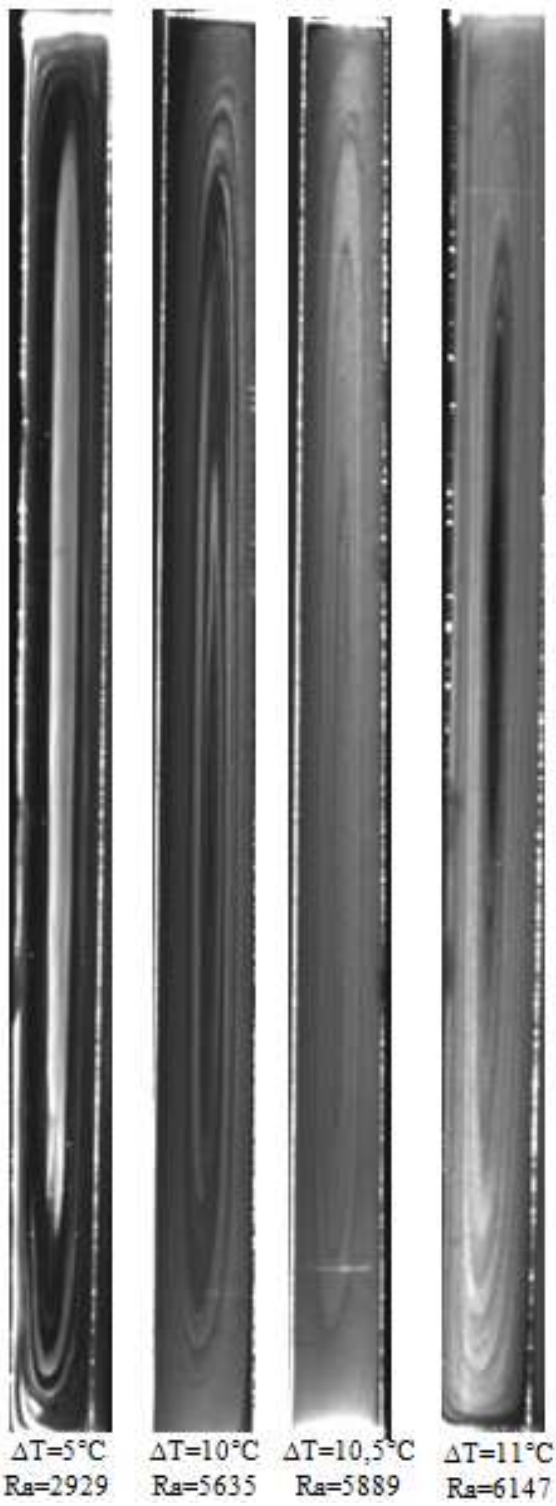


Figure 5. Flow patterns for different temperature difference and Rayleigh number.

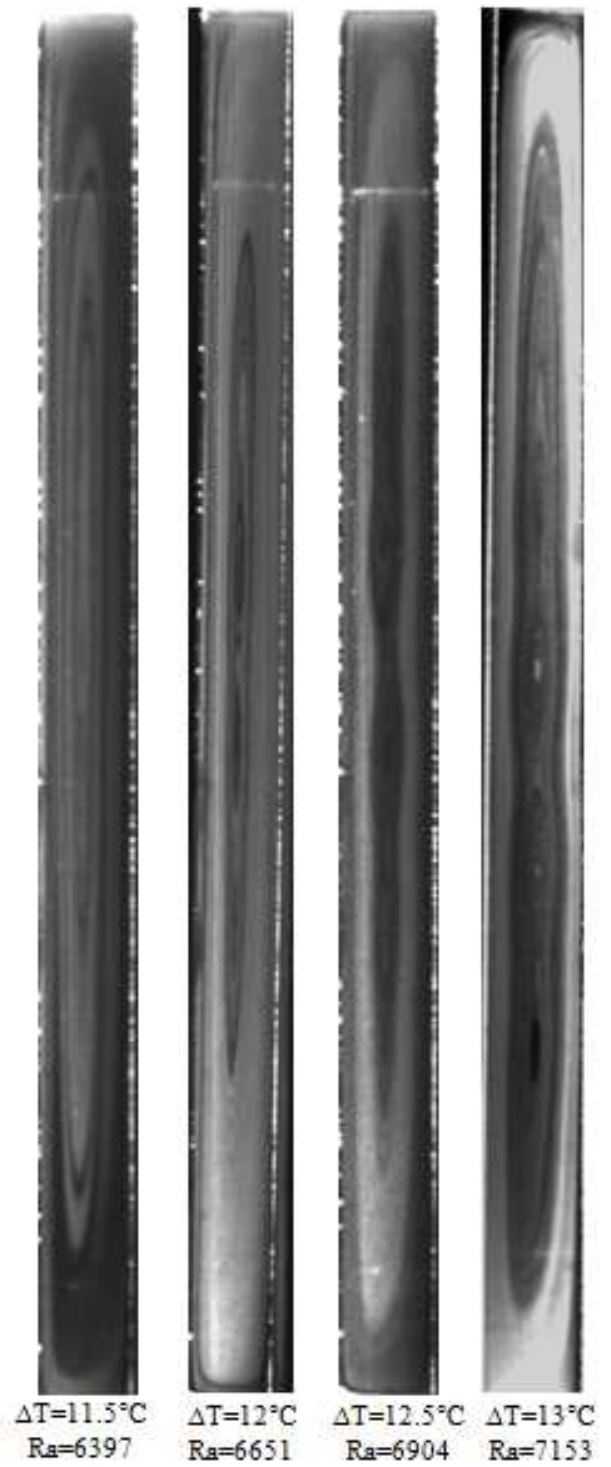


Figure 6. Flow patterns for different temperature difference and Rayleigh number.

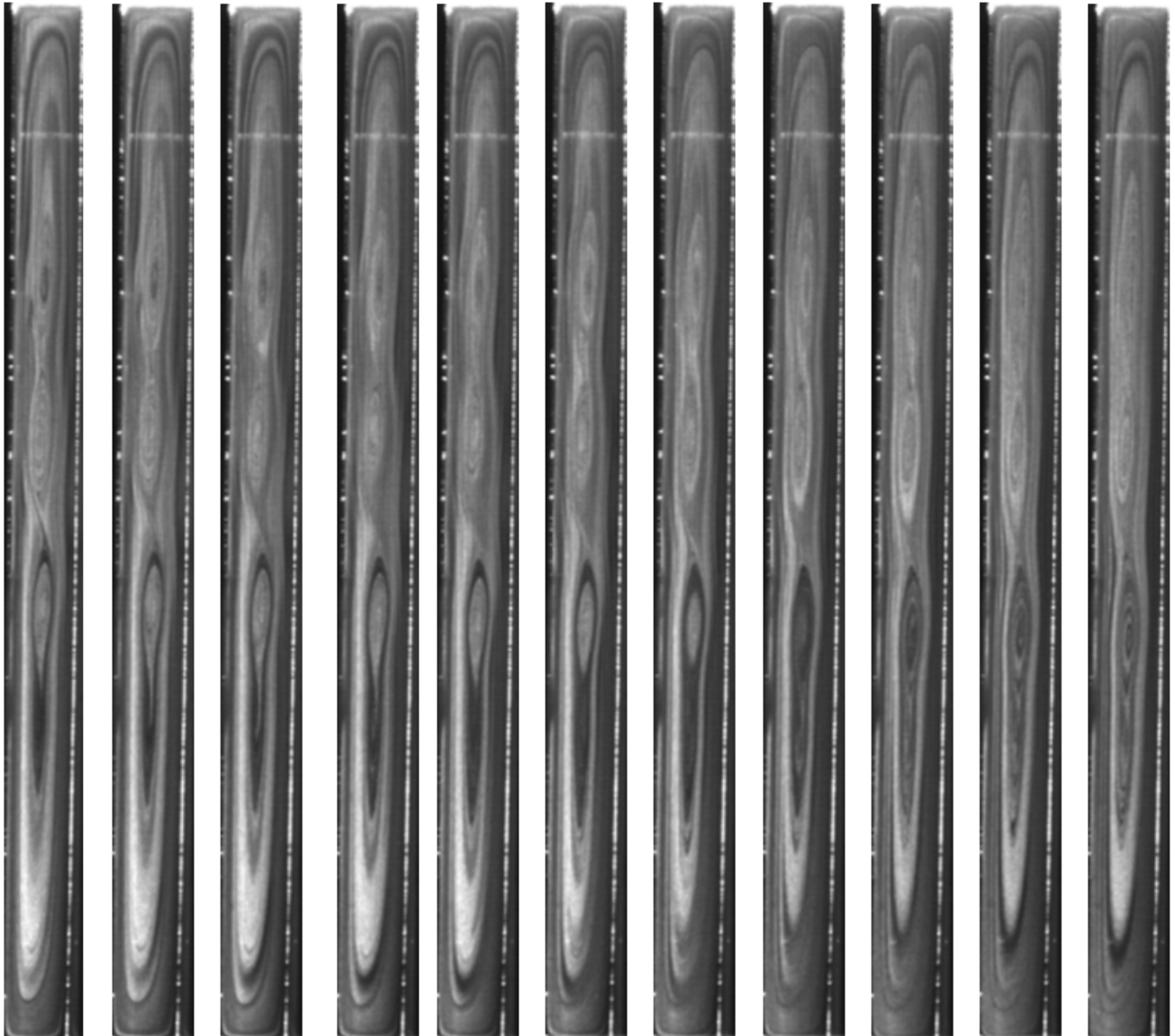


Figure 7. Sequence of flow growth inside the cavity for $Ra = 7402$ ($\Delta T = 13.5$ °C).

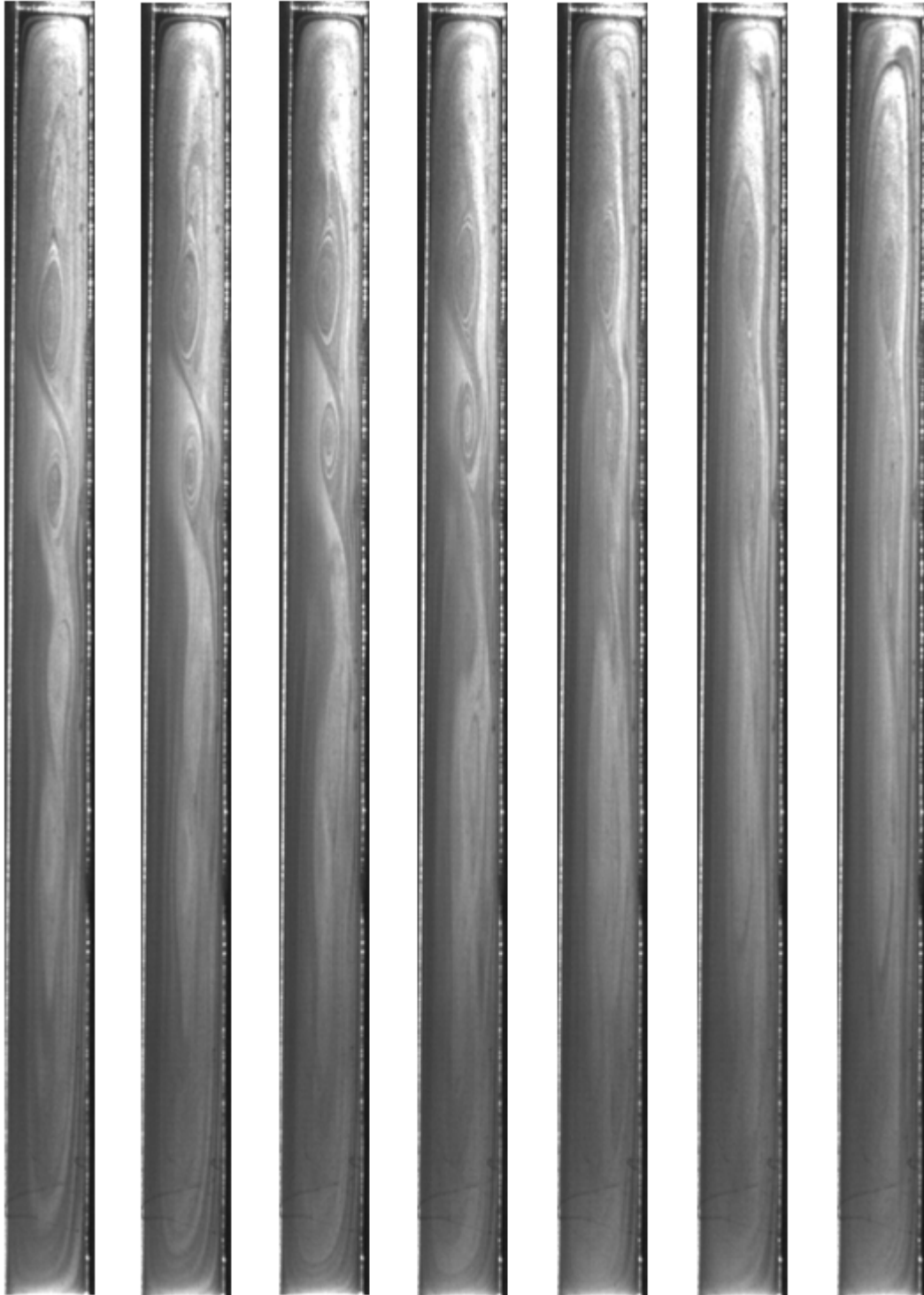


Figure 8. Flow growth inside the cavity for $Ra=8141$ ($\Delta T=15^\circ$).



Figure 9. Flow growth inside the cavity for $Ra=11772$ ($\Delta T=23^\circ\text{C}$).

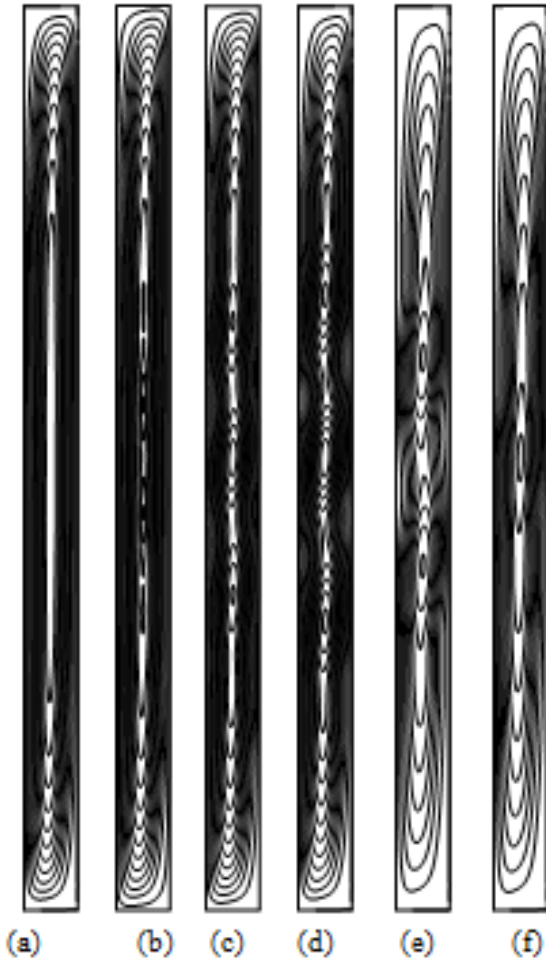


Figure 10. Numerical results of flow field contours inside the cavity for gradual heating at $H=15.5$, $Pr = 0.7$ for different Rayleigh number (a) 7000 ; (b) 7500 ; (c) 8000 ; (d) 12000 ; (e) 22000 ; (f) 25000.

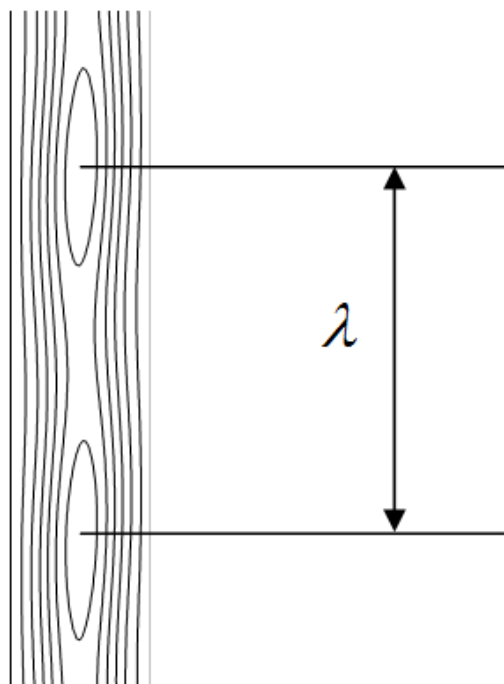


Figure 11. Wave lengths of the vortices.

Table 1 shows a comparison of wave number (α) between the experimental data of the present work and the results of Le Quéré [28] for a cavity of form factor ($H = 16$). The comparison is presented for two, three and four cells respectively. It can be observed an acceptable agreement between the present results and Le Quéré [28] results. Furthermore, it is observed that the difference between the present results and Le Quéré [28] results decreases as the cell number increases. The reason of this phenomenon can be go back to the friction effect in the core of the cavity and this effect decreases gradually as the number of cells increases and begin to grow. Table 2 shows the variation of the wave number computed experimentally and numerically according to Rayleigh number, for different temperature differences. It can be shown that the wave numbers increase as the Rayleigh number increases.

Table 1. Comparison of wave numbers between the experimental data of the present work and the results of Le Quéré [28].

Cells Number		4 cells	3 cells	2 cells
$\alpha = 2\pi / \lambda$	Le Quéré [28]	2.78	2.14	1.59
	Present Results	2.79	2.67	1.71

Table 2. Variation of the wave number according to Rayleigh number.

Experimental Results			
Ra (ΔT)	6651 (12 C°)	6904 (12,5 C°)	7153 (13 C°)
$\alpha = 2\pi / \lambda$	1.76	2.22	2.3
Numerical Results			
Ra	6651	6904	7153
$\alpha = 2\pi / \lambda$	1.84	2.34	2.77

5. Conclusions

As indicated above, the main aim of this work is to present the effects of Rayleigh number and temperature difference on flow field pattern in a two-dimensional transient flow in a differentially heated air-filled tall cavity. Some important findings can be drawn from the studied work as:

- The temperature increases when the time increases until it reaches the steady state.
- The convection circulation intensity increases as the Rayleigh number increases. In addition, the vortices are clearly elongated vertically inside the cavity zone.
- The results show that for Rayleigh numbers below $Ra = 7402$ ($\Delta T = 13.5^\circ C$), the flow pattern is permanent and approximately wavy.
- For Rayleigh numbers higher than 11772 ($\Delta T=23^\circ C$), the flow pattern becomes unstable and no reverse transition is observed.
- The number of flow vortices increase as the Rayleigh number increases.
- For high aspect ratios the flow characteristics are observed to be multi-cellular, have a sinusoidal profile and time variant.
- The nature of the flow instability changes with

increasing the temperature difference.

- When the Rayleigh number increases to about 6000, the flow becomes multi-cellular. Also, the transition to turbulent flow occurs at higher values of Rayleigh number.
- The direction of secondary cell movement is generally random.

Nomenclature

C_p Specific heat at constant pressure (kJ / kg. °C)

G Gravitational acceleration (m/s²)

H Cavity aspect ratio

k Thermal conductivity (W/ m. K)

L Cavity length (m)

Pr Prandtl number

Ra Rayleigh number

t Time

T Temperature (°C)

T_r Reference temperature (°C)

u Horizontal velocity component (m/sec)

v Vertical velocity component (m/sec)

w Cavity width (m)

x, y, z Cartesian coordinates (m)

Greek symbols

α Wave number

β Coefficient of thermal expansion (K⁻¹)

ρ Density (kg/m³)

μ Dynamic viscosity (kg /m.s)

λ Wave length of the vortices

ΔT Temperature difference

Subscripts

h hot

c cold

References

- [1] Bairi, A., Laraqi, N. and Garcia de Maria, J. Numerical and experimental study of natural convection in tilted parallelepipedic cavities for large Rayleigh numbers, *Experimental Thermal and Fluid Science*, Vol. 31, 2007, pp: 309–324.
- [2] Manca, O. and Nardini, S. Experimental investigation on natural convection in horizontal channels with the upper wall at uniform heat flux, *International Journal of Heat and Mass Transfer*, Vol. 50, 2007, pp: 1075–1086.
- [3] Fusegi, T. and Hyun, J. Laminar and transitional natural convection in an enclosure with complex and realistic conditions, *International Journal of Heat and Fluid Flow*, Vol. 15, 1994, pp: 258–268.
- [4] Khalifa, A. Natural convective heat transfer coefficient – A review. I. Isolated vertical and horizontal surfaces, *Energy Conversion and Management*, Vol. 42, 2001, pp: 491–504.
- [5] Khalifa, A. Natural convective heat transfer coefficient – A review. II. Surfaces in two and three-dimensional enclosures, *Energy Conversion and Management*, Vol. 42, 2001, pp: 505–517.
- [6] Turner, B. and Flack, R. The experimental measurements of natural convective heat transfer in rectangular enclosure with concentrated energy sources, *International Journal of Heat and Mass Transfer*, Vol. 102, 1980, pp: 236–241.
- [7] Fills, P. and Poulikakos, D. An experimental study of the effect of wall temperature non-uniformity on natural convection in an enclosure heated from the side, *International Journal of Heat and Fluid Flow*, Vol. 7, No. 4, 1986, pp: 258–265.
- [8] Tanasawa, I. Experimental techniques in natural convection, *Experimental Thermal and Fluid Science*, Vol.10, 1995, pp: 503–518.
- [9] Ramos, R. and Milanez, L. Numerical and experimental analysis of natural convection in cavity heated from below, *Proceedings of 11th IHTC*, Kyongju, Korea, 1998.
- [10] Salat, J., Xin, S., Joubert, P., Sergent, A., Penot, F. and Le Quere, P. Experimental and numerical investigation of turbulent natural convection in a large air-filled cavity, *International Journal of Heat and Fluid Flow*, Vol.25, 2004, pp: 824–832.
- [11] Bae, J. and Hyun, J. Time-dependent buoyant convection in an enclosure with discrete heat sources, *International Journal of Thermal Sciences*, Vol. 43, 2004, pp: 3–11.
- [12] Laguerre, O., Ben Amara, S. and Flick, D. Experimental study of heat transfer by natural convection in a closed cavity: application in a domestic refrigerator, *Journal of Food Engineering*, Vol. 70, 2005, pp: 523–537.
- [13] Corvaro, F. and Paroncini, M. Experimental analysis of natural convection in square cavities heated from below with 2D-PIV and holographic interferometry techniques, *Experimental Thermal and Fluid Science*, Vol. 31, 2007, pp: 721–739.
- [14] Laguerre, O., Ben Amara, S., Charrier-Mojtabi, M., Lartigue, B. and Flick, D. Experimental study of air flow by natural convection in a closed cavity: Application in a domestic refrigerator, *Journal of Food Engineering*, Vol. 85, 2008, pp: 547–560.
- [15] Corvaro, F. and Paroncini, M. An experimental study of natural convection in a differentially heated cavity through a 2D-PIV system, *International Journal of Heat and Mass Transfer*, Vol. 52, 2009, pp: 355–365.
- [16] Jeng, D., Yang, C. and Gau, C. Experimental and numerical study of transient natural convection due to mass transfer in inclined enclosures, *International Journal of Heat and Mass Transfer*, Vol. 52, 2009, pp: 181–192.
- [17] Corvaro, F., Paroncini, M. and Sotte, M. Experimental PIV and interferometric analysis of natural convection in a square enclosure with partially active hot and cold walls, *International Journal of Thermal Sciences*, Vol. 50, 2011, pp: 1629–1638.
- [18] Saury, D., Rouger, N., Djanna, F. and Penot, F. Natural convection in an air-filled cavity: Experimental results at large Rayleigh numbers, *International Communications in Heat and Mass Transfer*, Vol. 38, 2011, pp: 679–687.
- [19] Ivey, G. Experiments on transient natural convection in a cavity, *Journal of Fluid Mechanics*, Vol. 144, 1984, pp: 389–401.

- [20] Hess, C. and Henze, R. Experimental investigation of natural convection losses from open cavities, *Journal of Heat Transfer*, Vol. 106, 1984, pp: 333-338.
- [21] Kamotani, Y., Wang, L., Ostrach, S. and Jiang, H. Experimental study of natural convection in shallow enclosures with horizontal temperature and concentration gradients, *International Journal of Heat and Mass Transfer*, Vol. 28, 1985, pp: 165-173.
- [22] Cheesewright, R., King, K. and Ziai, S. Experimental data for the validation of computer codes for the prediction of two-dimensional buoyant cavity flows, In: *Notes on Numerical Flow Dynamics*, Vol. 60, ASME Winter Annual Meeting, 1986, pp: 75-81.
- [23] Upton, T. and Watt, D. Experimental study of transient natural convection in an inclined rectangular enclosure, *International Journal of Heat and Mass Transfer*, Vol. 40, No.11, 1997, pp: 2679-2690.
- [24] Upton, T. and Watt, D. Experimental study of transient natural convection in an inclined rectangular enclosure, *International Journal of Heat and Mass Transfer*, Vol. 40, No.11, 1997, pp: 2679-2690.
- [25] Betts, P. and Bokhari, I. Experiments on turbulent natural convection in a closed tall cavity, *International Journal of Heat and Mass Transfer*, Vol. 21, 2000, pp: 675-683.
- [26] Corvaro, F. and Paroncini, M. A numerical and experimental analysis on the natural convective heat transfer of a small heating heater located on the floor of a square cavity, *Applied Thermal Engineering*, Vol. 28, 2008, pp: 25-35.
- [27] Pons, M. The transition from single to multi-cell natural convection of air in cavities with an aspect ratio of 20, *Joint European Thermodynamics Conference IX*, France, 2007, pp: 150-154.
- [28] Le Quéré, P. A note on multiple and unsteady solutions in two-dimensional convection in a tall cavity, *ASME Journal of Heat Transfer*, Vol. 112, 1990, pp: 965-974.